ISSN 1063-7788, Physics of Atomic Nuclei, 2024, Vol. 87, No. 1, pp. 44–48. © Pleiades Publishing, Ltd., 2024.

ELEMENTARY PARTICLES AND FIELDS
Experiment

The pp-Scattering Simulation for the Beam–Beam Counter at SPD, NICA

A. A. Terekhin[1)*], V. V. Abramov[2)], V. P. Ladygin[1)], J. Kurmanaliev[1)], and I. S. Volkov[1)]

Received November 13, 2023; revised November 13, 2023; accepted November 13, 2023

Abstract—The article presents the results of the pp-scattering simulation at the total energy up to 27 GeV for the SPD Technical Design Report version of the Beam–Beam Counter. In the SPDRoot framework the simulation has been performed using the event generators: FRITIOF, Pythia8, and Pluto. The results have been compared with the differential cross section of the existing experimental data. The first estimations of the inclusive charged particle production asymmetries with Beam–Beam Counter have been obtained.

DOI: 10.1134/S1063778824020170

1. INTRODUCTION

The polarized experiments are the important part of the modern particle physics. The research of the pp-, dd- and pd-collisions is essential tool for precise understanding the spin dependence of the nucleon–nucleon strong interactions. NICA (Nuclotron based Ion Collider fAcility), which is under construction, will allow one to perform measurements at the total energy up to $\sqrt{s} = 27$ GeV. Spin Physics Detector (SPD) [1] will be placed in one of the two beam collision points of the NICA. This detector is being developed as a universal setup for the comprehensive study of gluons in protons and deuterons at the luminosity up to 10^{32} cm^{-2} s^{-1}. It is planned to measure the single and double asymmetries in the production of the charmonia, open charm, and prompt photons. The SPD experimental setup is designed as a universal 4π detector with advanced tracking and particle identification. It includes: a vertex detector, a straw-tube based tracking system, a time-of-flight system, an aerogel-based Cherenkov detector, an electromagnetic calorimeter, a muon (range) system, beam–beam counters (BBC), and zero-degree calorimeters. Two BBC are designed to perform the local polarimetry of the transverse polarized protons and control the luminosity of the beam collision.

The paper gives the simulation results of the pp-scattering at the energies $\sqrt{s} = 6.2$, 10 and 23.5 GeV for the BBC under SPDRoot [2] framework.

[1)]Joint Institute for Nuclear Research, Dubna, Russia.
[2)]National Research Centre Kurchatov Institute—IHEP, Protvino, Russia.
[*]E-mail: aterekhin@jinr.ru

2. BEAM–BEAM COUNTER

The SPD will include two beam–beam counters. In the current design the BBC consists of ∼96 scintillation tiles. It will be divided into 6 concentric layers with 16 azimuthal sectors each. The distance between the tiles is equal to 10 mm. The tile thickness is equal to 5 mm. Due to azimuthal granulation, they can be used to determine and control the beam polarization via the measurement of the single-spin asymmetry in the elastic pp- and dd-scattering. It is necessary to control the beam polarization during data taking to reduce the systematic error caused by varying the beam polarization. At NICA energies the value of the inclusive single-spin asymmetry is expected to be significant [3]. Therefore, the BBC can be used for the local polarimetry at SPD.

The diameter of BBC will be equal to approximately 1700 mm. The distance between each detector and SPD center is equal to $Z = 1716$ mm. The above BBC configuration allows one to cover the angle scattering range up to $\theta = 25^\circ{-}30^\circ$. The uncertainty of the interaction point location is expected to be $\Delta Z \sim \pm 300$ mm. The wavelength shifting (WLS) fiber will be installed in each BBC tile. The tiles of the BBC are observed by the silicon photomultiplier (SiPMs). The measurement of the signal amplitude is required for the time-walk correction to improve the time resolution.

3. SIMULATION OF THE pp-SCATTERING

The BBC geometry was used to simulate the pp-scattering. The simulation at energies $\sqrt{s} = 6.2$, 10 and 23.5 GeV has been performed by using the FRITIOF (FTF) and Pythia8 generators within the SPDroot framework. The events' distributions have

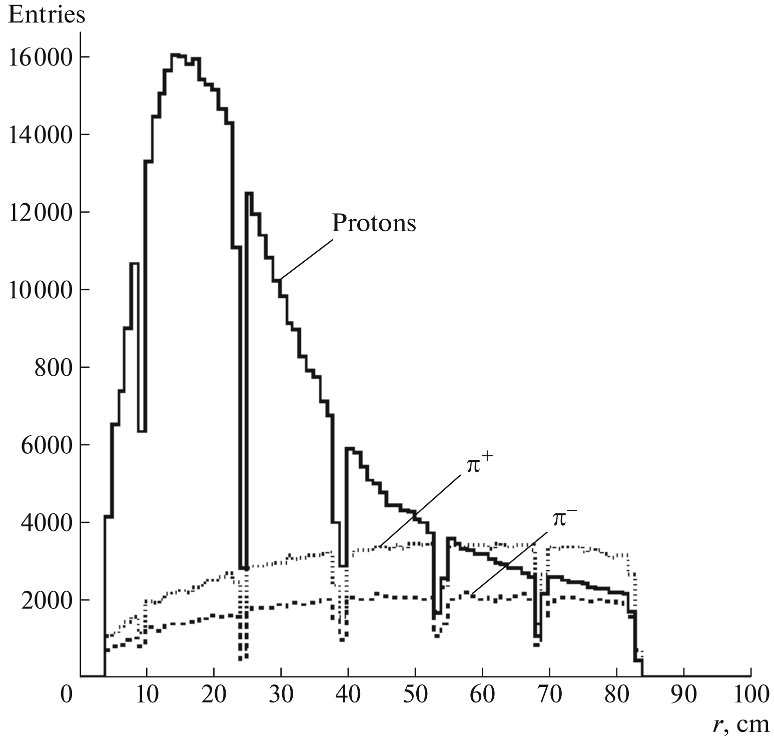

Fig. 1. The entries' distributions as a function of the BBC plane radius for protons, π^+, and π^- particles, shown with the solid, dotted and dashed lines, respectively. The results have been obtained using FTF generator at total energy $\sqrt{s} = 6.2$ GeV.

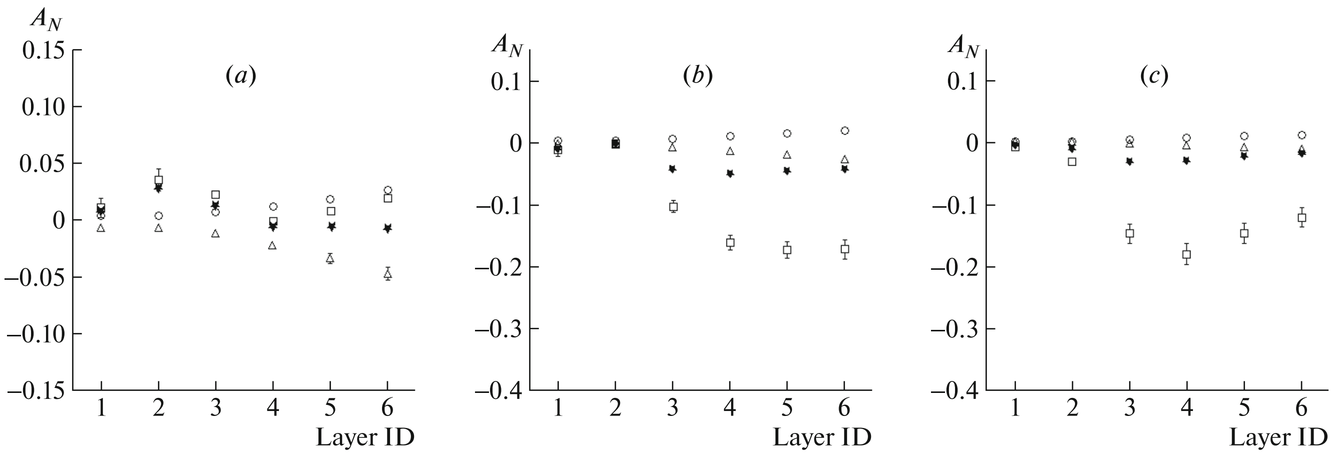

Fig. 2. The analyzing powers A_N and A_N^{eff} obtained within the framework of the model CPQ using the FTF—simulation results. (a), (b) and (c) results of the calculations at energies $\sqrt{s} = 6.2$, 10 and 23.5 GeV, respectively. The open triangles, circles, and squares are the A_N data for protons, π^+, and π^-, respectively. The solid stars are the A_N^{eff} data.

been obtained as dependence on radius (r) in the BBC plane for protons, π^+, and π^- particles. The r-dependencies obtained by means of the FTF—events generator at 6.2 GeV are demonstrated in Fig. 1. The data for the protons, π^+, and π^- particles are shown with the solid, dotted and dashed lines, respectively. Also, the comparison of the Feynman variable x_F- and the transverse momentum p_t-distributions has been performed with the FTF and Pythia8 generators. The both generators have given similar results.

The analyzing powers A_N for inclusive reaction have been calculated within the framework of the phenomenological model for chromomagnetic polarization of quarks (CPQ) [3]. The efficient analyzing

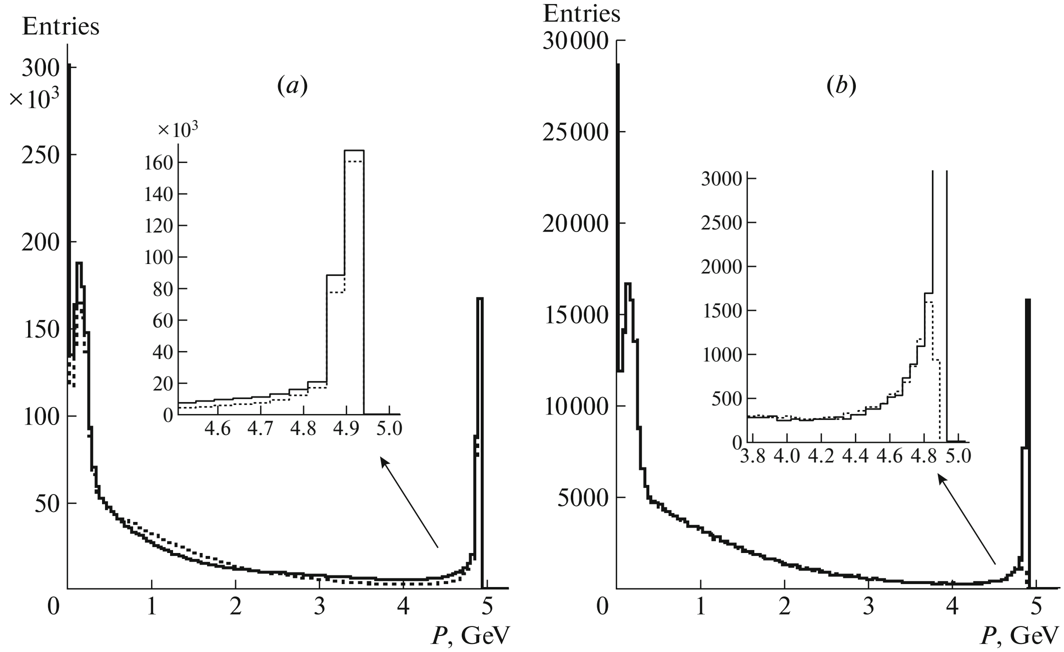

Fig. 3. (a) The momentum P distribution of all charged particles at the energy 10 GeV obtained with the Pythia8 generator. The results with elastic scattering turning on and off are shown with the solid and dashed histograms, respectively. (b) the P-distributions obtained at 10 GeV with the FTF (solid histogram) and Pythia8 (dashed histogram) generators.

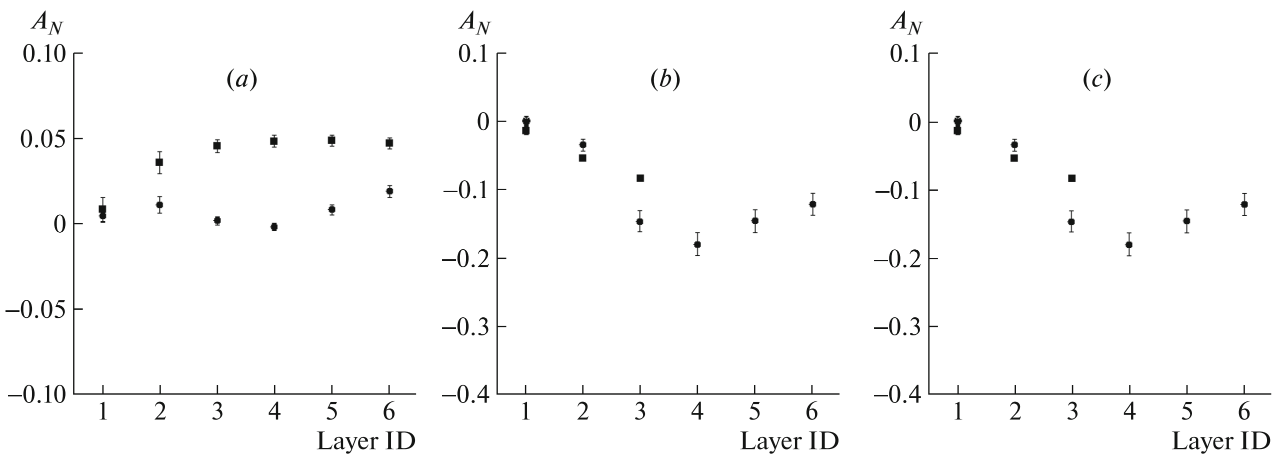

Fig. 4. The analyzing powers A_N have been calculated at the energies 6.2 (a), 10 (b) and 23.5 (c) GeV using the FTF generator. The data for elastic and inelastic scattering are shown with the squares and circles, respectively.

powers A_N^{eff} have been estimated by the formula:

$$A_N^{\text{eff}} = \frac{A_N^p N_p + A_N^{\pi^+} N_{\pi^+} + A_N^{\pi^-} N_{\pi^-}}{N_{\text{ch}}}. \qquad (1)$$

Here N_{ch} is the total charged particle number, N_p, N_π^+, N_π^-—number of the protons, π^+, and π^- in each circle layer. The calculated values of the A_N and A_N^{eff} using the FTF-simulation results are demonstrated in Fig. 2. The value of asymmetry A_N^{eff} is small due to the small values of x_F and p_t in this kinematic area. The non-zero value for second (and third) sector is due to the A_N^{proton} (elastic or inelastic scattering).

Also, the asymmetry estimation has been obtained for 10 and 23.5 GeV. At $\sqrt{s} > 10$ GeV the A_N^{eff} has non-zero values for the layers number >2. The selection of the elastic channel is necessary to estimate its contribution to the behavior of A_N^{eff}. The analysis of the momentum distributions for all particles has been performed for this purpose. The obtained results at 10 GeV using the FTF and Pythia8 are shown in Fig. 3a with the solid and dashed histograms, respec-

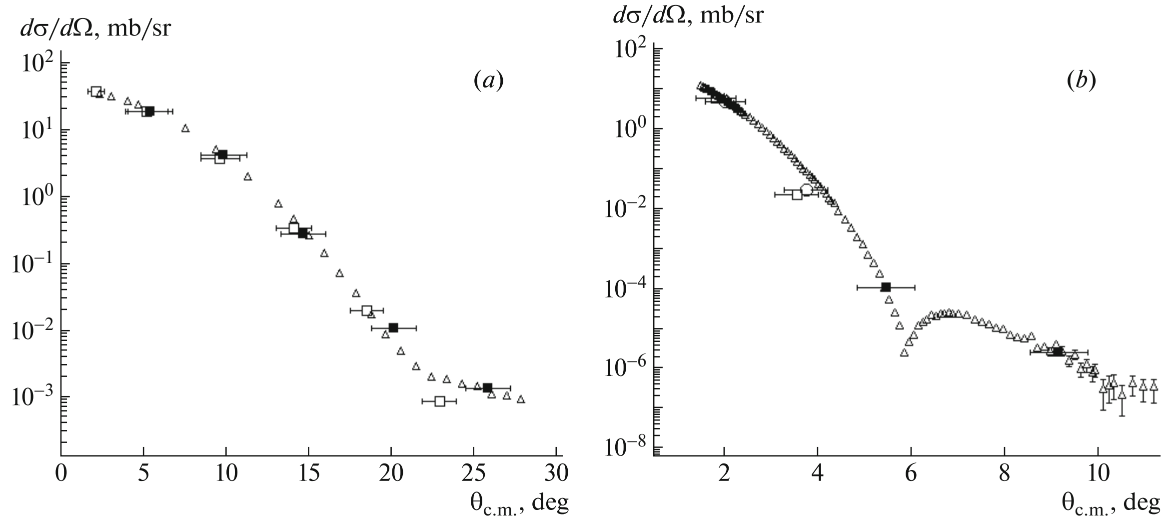

Fig. 5. The angular dependencies of the differential cross section (triangles) and simulation results. The simulation data with the FTF, Pythia8 and Pluto generators are shown with the open squares, circles, and solid squares, respectively. (a) the data at $\sqrt{s} = 6.2$ GeV, (b) the data at $\sqrt{s} = 23.5$ GeV.

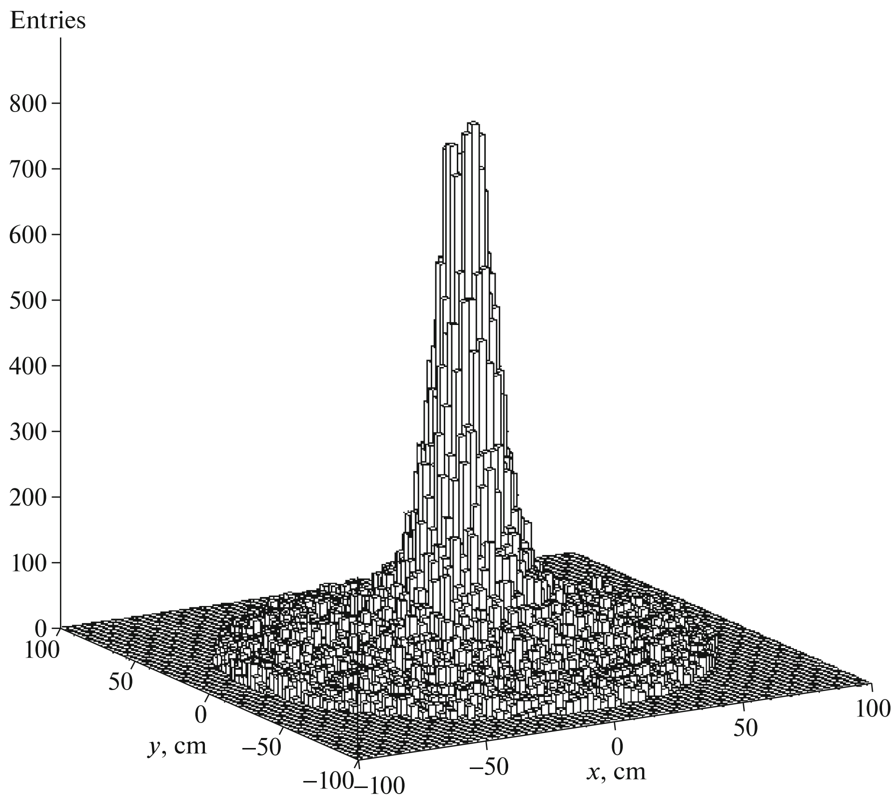

Fig. 6. The radial (r) event dependence in the BBC plane at the energy 10 GeV obtained with the Pythia8 generator.

tively. The both generators have given the similar results. The momentum distributions of all charged particles with and without account of the pp-elastic scattering are illustrated in Fig. 3b with the solid and dashed histograms, respectively. The data have been obtained using the Pythia8 generator. The analysis of these distributions has shown that the elastic events are concentrated at the $P > 4.85$ GeV/c. The elastically scattered protons can be selected from the total number of particles by means of the cut on the momentum P. The analyzing powers A_N have been calculated at three energies (6.2, 10 and 23.5 GeV) for pp-elastic and inelastic scattering (Fig. 4). The elastic scattering plays a significant role at all layers (except for the first one) at the energy 6.2 GeV. The contribution of the inelastic scattering is close to zero at this energy. The role of the inelastic channel is important starting from the third layer at 10 and 23.5 GeV. The contribution of the elastic scattering is approximately equal to zero and decreases with the energy increasing because of the strong fall of the pp-elastic scattering differential cross section at high energies. Thus, the elastic scattering plays an important role at the $\sqrt{s} < 10$ GeV. The pp-inelastic scattering, on the contrary, is significant at the $\sqrt{s} >$ 10 GeV.

The angular dependencies of the obtained normalized elastic scattering events have been compared with the differential cross section at the similar energies [4, 5]. The data at energies $\sqrt{s} = 6.2$ and 23.5 GeV are presented in Fig. 5. The normalized yields of the pp-elastic events obtained earlier [6] with the Pluto generator [7] are shown with the solid squares. The simulation results are in agreement with the behavior of the experimental data.

A new BBC geometry was offered with an increased number of tiles. Each azimuthal sector includes 25 tiles, inside which the WLS will be installed. The opening angle of the sector is the same (22°). The distance between the tiles is equal to 1 mm. The tile is 10 mm thick. Such design will increase light collection. The new geometry has been implemented within SPDroot framework. The momentum P, Feynman variable x_F, the transverse momentum p_t-distributions and the radial (r) event dependence in the BBC plane have been obtained. As example the r-distribution at the energy 10 GeV obtained with the Pythia8 generator is shown in Fig. 6

4. CONCLUSIONS

The simulation of the pp-scattering at the energy $\sqrt{s} < 27$ GeV has been performed for SPD BBC using the FTF, Pythia8, and Pluto generators within SPDroot framework.

The efficient analyzing powers A_N have been estimated for pp-interaction at $\sqrt{s} = 6.2$, 10 and 23.5 GeV within the framework of the phenomenological model for chromomagnetic polarization of quarks [3].

The role of the pp-elastic scattering has been studied. It has shown that the elastic channel gives significant contribution to the efficient asymmetry at the energy $\sqrt{s} < 10$ GeV. The inelastic channel, on the contrary, gives a significant contribution at the energy $\sqrt{s} > 10$ GeV.

The comparison of the simulation results with the differential cross section experimental data has been performed. The data are in agreement.

The work with the new highly granular design of the BBC has been started.

FUNDING

This work was partially supported by a grant no. 22-12-00164 from the Russian Science Foundation.

CONFLICT OF INTEREST

The authors of this work declare that they have no conflicts of interest.

REFERENCES

1. V. M. Abazov, V. Abramov, L. G. Afanasyev, R. R. Akhunzyanov, A. V. Akindinov, N. Akopov, I. G. Alekseev, A. M. Aleshko, V. Yu. Alexakhin, G. D. Alexeev, M. Alexeev, A. Amoroso, I. V. Anikin, V. F. Andreev, V. A. Anosov, A. B. Arbuzov, et al., arXiv Preprint (2021). https://doi.org/10.48550/arXiv.2102.00442
2. spdroot: Offline framework for the SPD experiment. https://git.jinr.ru/nica/spdroot.
3. V. V. Abramov, JPS Conf. Proc. **37**, 020901 (2022). https://doi.org/10.7566/JPSCP.37.020901
4. J. V. Allaby, F. G. Binon, A. N. Diddens, P. Duteil, A. Klovning, R. Meunier, J. P. Peigneux, E. J. Sacharidis, K. Schlüpmann, M. Spighel, J. P. Stroot, A. M. Thorndike, and A. M. Wetherell, Phys. Lett. B **28**, 67 (1968). https://doi.org/10.1016/0370-2693(68)90545-5
5. Z. Asa'd, C. Baglin, S. Benson, R. Böck, K. Brobakken, L. Bugge, T. Buran, A. Buzzo, P. J. Carlson, M. Coupland, D. G. Davis, B. G. Duff, S. Ferroni, I. Gjerpe, V. Gracco, J. D. Hansen, P. Helgaker, F. F. Heymann, D. C. Imrie, T. Jacobsen, K. E. Johansson, K. Kirsebom, R. Lowndes, A. Lundby, G. J. Lush, M. Macri, R. Møllerud, J. Myrheim, M. H. Phillips, M. Poulet, L. Rossi, A. Santroni, G. Skjevling, S. O. Sørensen, and M. Yvert, Phys. Lett. B **108**, 51 (1982). https://doi.org/10.1016/0370-2693(82)91140-6
6. A. A. Terekhin, V. P. Ladygin, A. Y. Isupov, I. S. Volkov, S. G. Reznikov, Y. V. Gurchin, A. V. Tishevsky, and K. S. Legostaeva, Bull. Russ. Acad. Sci.: Phys. **87**, 1166 (2023). https://doi.org/10.3103/s1062873823703045
7. F. Dohrmann, I. Fröhlich, T. Galatyuk, R. Holzmann, P. K. Kählitz, B. Kämpfer, E. Morinière, Y. C. Pachmayer, B. Ramstein, P. Salabura, J. Stroth, R. Trebacz, J. Van de Wiele, and J. Wüstenfeld, Eur. Phys. J. A **45**, 401 (2010). https://doi.org/10.1140/epja/i2010-11012-3